Journal of Mechanical Design. Received June 20, 2023;
Accepted manuscript posted October 11, 2023. doi:10.1115/1.4063824

Designing Mixed-Category Stochastic Microstructures by Deep Generative Model-based and Curvature Functional-based Methods

Leidong Xu, Kiarash Naghavi Khanghah, Hongyi Xu*

Mechanical Engineering, University of Connecticut, Storrs, CT, USA 06269

* Email: hongyi.3.xu@uconn.edu

ABSTRACT

Bridging the gaps among various categories of stochastic microstructures remains a challenge in the design representation of microstructural materials. Each microstructure category requires certain unique mathematical and statistical methods to define the design space (design representation). The design representation methods are usually incompatible between two different categories of stochastic microstructures. The common practice of pre-selecting the microstructure category and the associated design representation method before conducting rigorous computational design restricts the design freedom and hinders the discovery of innovative microstructure designs. To overcome this issue, this paper proposes and compares two novel methods, the deep generative modeling-based method and the curvature functional-based method, to understand their pros and cons in designing mixed-category stochastic microstructures for desired properties. For the deep generative modeling-based method, the Variational Autoencoder is employed to generate an unstructured latent space as the design space. For the curvature functional-based method, the microstructure geometry is represented by curvature functionals, of which the functional parameters are employed as the microstructure design variables. Regressors of the microstructure design variables-property relationship are trained for microstructure design optimization. A comparative study is conducted to understand the relative merits of these two methods in terms of computational cost, continuous transition, design scalability, design diversity, dimensionality of the design space, interpretability of the statistical equivalency, and design performance.

Keywords: Stochastic microstructures; Metamaterials; Deep generative model; Curvature functional; Design representation.

1. INTRODUCTION

By designing the microstructures of architected materials, a wide spectrum of properties, such as strength [1-3], ductility [4], energy density [5, 6], and thermal conductivity [1, 7, 8], can be achieved to meet engineering requirements. Here we focus on stochastic microstructures, of which the statistical variations in structural characteristics are induced by uncertainties in the manufacturing processes [9-11], defects or porosities [12], or the inherent randomness at the micro- or nano-scale [13, 14]. In the field of engineered architected metamaterials, designers have looked into stochastic structure designs to achieve higher energy absorption [6, 15, 16], compatibility with traditional manufacturing techniques [17, 18], and robustness against defects [19].

In the literature, a variety of statistical characterization and stochastic reconstruction-based approaches have been proposed for designing stochastic microstructures. Statistical characterization is a process that generates statistical descriptors and functions of the stochastic microstructure features observed from digital images (e.g., microscopic images). Stochastic reconstruction is a process that re-generates statistically equivalent microstructures based on the input statistical descriptors and functions. One simple and

Journal of Mechanical Design. Received June 20, 2023;
Accepted manuscript posted October 11, 2023. doi:10.1115/1.4063824

straightforward way is to characterize microstructures with physically meaningful parametric descriptors such as volume fraction, particle/pore size, fiber length, fiber orientation, etc. In addition, high dimensional statistical functions including *N*-point correlation functions [20-23], spectrum density function [24, 25], and random fields [26, 27] have also been applied to describe the complex stochastic microstructure morphologies. One major limitation of these methods is that each stochastic microstructure category requires some unique mathematical and statistical representations that are incompatible with other categories. For example, random fiber composites require fiber orientation tensor [10, 28], random particle composites require the statistical distribution of particle diameters [29, 30], granular alloy microstructures require both grain orientation and crystal orientation [31], and spinodal-like structures can be described with spectrum density function [25]. Therefore, a designer needs to decide the microstructure category before defining the design space and conducting computational design. The step of pre-selecting the microstructure category limits the design freedom and reduces the possibility of obtaining innovative microstructure designs.

In recent years, deep generative models, such as Variational Autoencoders (VAEs), generative adversarial networks (GANs), diffusion model, and their variations, have been employed in stochastic microstructure reconstruction and design [16, 32-39]. However, the aforementioned works only consider a limited number of microstructure categories [40] and do not focus on bridging the gaps among various categories. In our previous work [41], we established a deep generative modeling framework that learns a unified microstructure design space based on multiple categories of stochastic microstructures (random fibers, random particles, random ellipses, random node-edge networks, and random amorphous microstructures) and deterministic, periodic microstructures (e.g., cellular metamaterials). This framework enables a smooth transition between stochastic and deterministic structural patterns in the property-driven microstructure design. However, this framework only handles 2D microstructure images and is demanding on training data and computational resources, so its application to 3D microstructure design is limited by the curse of dimensionality.

To address the aforementioned challenges, here we establish two approaches that have the capability of generating a unified design space that embodies various categories of stochastic microstructures:

(i) A data-driven approach based on the deep generative model;

(ii) A mathematics-based approach that is established upon the curvature functionals.

As shown in Figure 1, these two methods are employed in design representation to create a parametric design space for stochastic microstructure design. With the obtained design space, Design of Experiments (DOE), supervised learning of the microstructure-property relationship, and property-driven design will be conducted to generate new microstructure designs. A comparative study will be presented to discuss the pros and cons of the two methods.

The remainder of the paper is organized as follows. Section 2 introduces the deep generative model-based design methodology. Section 3 introduces the curvature functional-based design methods. In section 4, a microstructure design case is presented to compare the two methods. Section 5 presents a comprehensive discussion of the comparison of the two methods. Section 6 concludes this paper.

Journal of Mechanical Design. Received June 20, 2023;
Accepted manuscript posted October 11, 2023. doi:10.1115/1.4063824

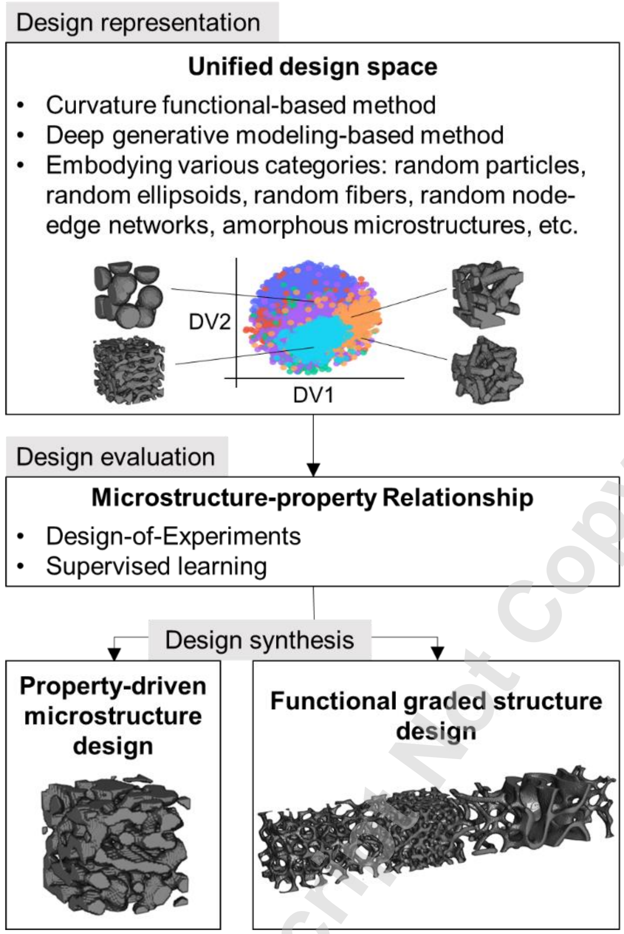

Figure 1: Design of mixed-category stochastic microstructures. A curvature functional-based method and a deep generative model-based method are proposed and compared. Both methods are employed to create a unified design space that embodies various categories of stochastic microstructures for the property-driven microstructure design.

2. DEEP GENERATIVE MODEL-BASED METHOD

One way to bridge the gap among different microstructure categories is to leverage the data-driven approach, e.g., deep feature learning, to learn a unified design space based on a large and diverse microstructure database that embodies various categories of microstructures. We first established a 3D stochastic microstructure database by leveraging the stochastic reconstruction methods proposed in our previous works, including the statistical descriptor-based method [10, 30, 42, 43], the space tessellation-based method [9], the spectrum density function (SDF)-based random field method [14], etc. This database consists of 40,000 microstructural images with a resolution of 64×64×64, and the microstructure samples can be classified into five categories: random particles, random fibers, random ellipsoids, random node-edge networks, and amorphous microstructures. Each category includes 8,000 microstructural images with varying statistical descriptor values, such as fiber lengths and diameters for the random fiber samples and spectrum density functions for the random amorphous microstructures. Samples from each category are shown in Figure 2. The dataset is divided into a training set and a test set in a ratio of 9:1.

Journal of Mechanical Design. Received June 20, 2023;
Accepted manuscript posted October 11, 2023. doi:10.1115/1.4063824

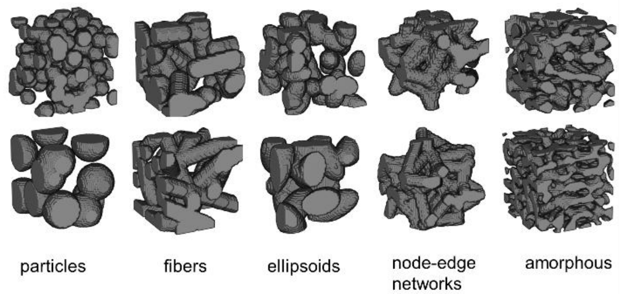

Figure 2: Examples of microstructure samples in the database for deep generative modeling. From left to right: random particles, random fibers, random ellipsoids, random node-edge networks, and amorphous microstructures.

2.1. Microstructure representation by VAE

VAE is a deep generative model that consists of two major components: an encoder network and a decoder network. The encoder network maps the input data to a Gaussian distribution in the latent space, which allows for the generation of novel data samples through sampling from the learned distribution. The decoder network takes the latent representation as the input and reconstructs the original data. The key feature of VAE is the introduction of a probabilistic approach to encode the input data into the latent space. Rather than mapping the input data to a single point in the latent space, the VAE maps the input data to a probability distribution over the latent space. Compared to other generative models, e.g., GAN and diffusion model, VAE provides an interpretable latent space, which can be used as a low-dimensional design space. The similarity of structural features can be measured by the distance in the latent space of VAE. Moreover, GAN models encounter several training instability issues, including diminished gradient and model collapse, which limit their application to complex datasets. In order to tackle those challenges, we employed a WGAN [44] model to enhance training stability and encourage model convergence. However, it is observed that the synthetic images generated by WGAN displayed reduced diversity compared to those generated by the VAE model. The generator of WGAN tends to generate microstructure images by blending patterns and styles from the provided microstructure dataset. A comparison of synthetic images generated by GAN and VAE can be found in the Appendix. A1. It is worth noting that despite the improved stability and convergence achieved by the WGAN model, it requires a greater number of epochs and more time to reach convergence compared to the VAE model. As a result, the VAE model was chosen for this study.

A general loss function of a vanilla VAE is expressed as:

$$L_i(\boldsymbol{\theta}, \boldsymbol{\phi}) = -E_{z\sim q_{\theta}(\boldsymbol{z}|\boldsymbol{x}_i)}\left[log\, \boldsymbol{p}_{\boldsymbol{\phi}}\left(\boldsymbol{x}_i \mid \boldsymbol{z}\right)\right] + D_{KL}\left(\boldsymbol{q}_{\boldsymbol{\theta}}\left(\boldsymbol{z} \mid \boldsymbol{x}_i\right)\middle|\boldsymbol{p}(\boldsymbol{z})\right) \quad (1)$$

where $\boldsymbol{\theta}$ and $\boldsymbol{\phi}$ are the parameters of the decoder and encoder, respectively, and $\boldsymbol{x}_i$ is input microstructure image data for our case, and $\boldsymbol{z}$ denotes the latent vectors. The first term, $-E_{\boldsymbol{z}\sim \boldsymbol{q}_{\boldsymbol{\theta}}(\boldsymbol{z}|\boldsymbol{x}_i)}\left[log\, \boldsymbol{p}_{\boldsymbol{\phi}}\left(\boldsymbol{x}_i \mid \boldsymbol{z}\right)\right]$, is the reconstruction loss that measures the pixel-level error between the input and reconstruction. The second term, $D_{KL}\left(\boldsymbol{q}_{\boldsymbol{\theta}}\left(\boldsymbol{z} \mid \boldsymbol{x}_i\right)\middle|\boldsymbol{p}(\boldsymbol{z})\right)$, denotes the KL loss and ensures that the learned distribution q follows the true prior distribution p. Practically, including the KL term in the loss function can avoid overfitting and also regularize the latent space to reduce discontinuities in the latent space.

Journal of Mechanical Design. Received June 20, 2023;
Accepted manuscript posted October 11, 2023. doi:10.1115/1.4063824

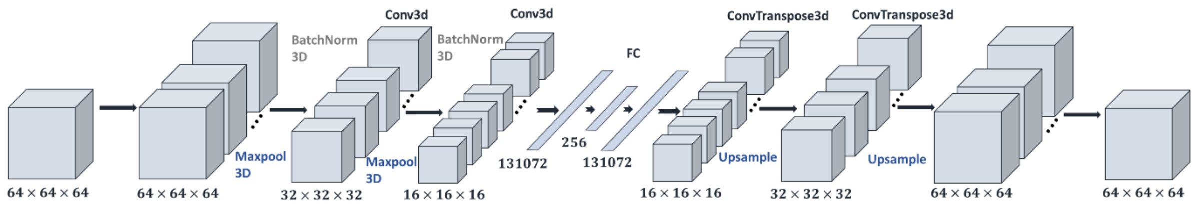

Figure 3: Architecture of the Variational Autoencoder. The reduced dimensional latent space is employed as the design space.

Figure 3 shows our implementation of the VAE to generate a parametric latent space representation of the stochastic microstructures as the design space. The encoder follows a VGG-style architecture, in which the convolution layer blocks are followed by the fully connected layers. The dimension of latent vectors is set at 256 based on the results of trials, in order to balance the reconstruction quality and the time efficiency of conducting optimal microstructure search in the latent space. The VAE model was trained by 150 epochs, and the training history is shown in Figure A2 at Appendix. To improve the reconstruction quality and address the KL vanishing problem, we implemented the monotonic annealing schedule for KL loss [45]. The reconstruction error for each category of microstructure is shown in Table A.2 in appendix.

We also explored other variants of VAE in this work. Literature and our previous work suggest that including a style loss term in the loss function typically enhances reconstruction quality significantly [41, 46]. However, the small improvement in quality comes at the cost of a substantial increase in computational complexity due to the tensor permutation process on each image in all three directions. We also tested an architecture that incorporates the style loss [46], but did not observe an improvement in the reconstruction quality. Furthermore, we experimented with a Gaussian-mixture VAE [47], but did not observe any significant benefits either. After a thorough exploration of these options, we decided to employ a vanilla VAE for its computational efficiency.

2.2 Property-driven microstructure design and generation of functionally graded structure designs by VAE

As discussed in Section 1, we adopt the surrogate model-based optimization approach to design microstructures for desired properties. The latent variables are considered as microstructure design variables. DOE is conducted in latent space to generate a dataset for training the microstructure-property surrogate models. Multi-response Gaussian Process (GP) regression models are employed to establish the relationship between the latent variables and the mechanical properties.

As the computational cost of design evaluation (by surrogate model) during the optimization process is not a concern here, we select the Genetic Algorithm (GA) to solve the design problem. GA, and other evolutionary algorithms, have the advantage of avoiding local minima. For multi-objective optimization problems, Non-dominated Sorting Genetic Algorithm II (NSGA-II) [48] is employed as the optimizer.

The optimal designs are first obtained in the format of latent vector, and the corresponding microstructure images are reconstructed by the decoder. The properties of the optimal microstructure designs are verified by simulations, as there always exist discrepancies between the surrogate model-predicted properties and the true values.

In addition to designing microstructure units, we also investigate the VAE model's capability of generating functionally graded structure designs. A functionally graded structure is characterized by the variation in structure gradually over volume, resulting in corresponding continuous changes in the properties. A series of microstructure units are generated by conducting spherical linear interpolation [49] between two microstructure unit samples in the latent space. A gradual change in the microstructure features

Journal of Mechanical Design. Received June 20, 2023;
Accepted manuscript posted October 11, 2023. doi:10.1115/1.4063824

can be observed in this series of designs. A functionally graded structure can be generated by assembling those microstructure units sequentially (Figure 4). Due to the discrete nature of the microstructure interpolation, one outstanding shortcoming is the lack of continuity at the interface between two adjacent microstructure units. The presence of discontinuities at the interface can lead to local stress concentrations that may weaken the overall strength of the structure and even cause it to failure. Non-smooth transitions in the interfaces can be observed, as shown in the side views in Figure 4 (d). It is to be noted that the purpose of creating this series of cells is solely to illustrate the discontinuity issue at the interface between two adjacent cells, rather than being a process driven by the generation of properties.

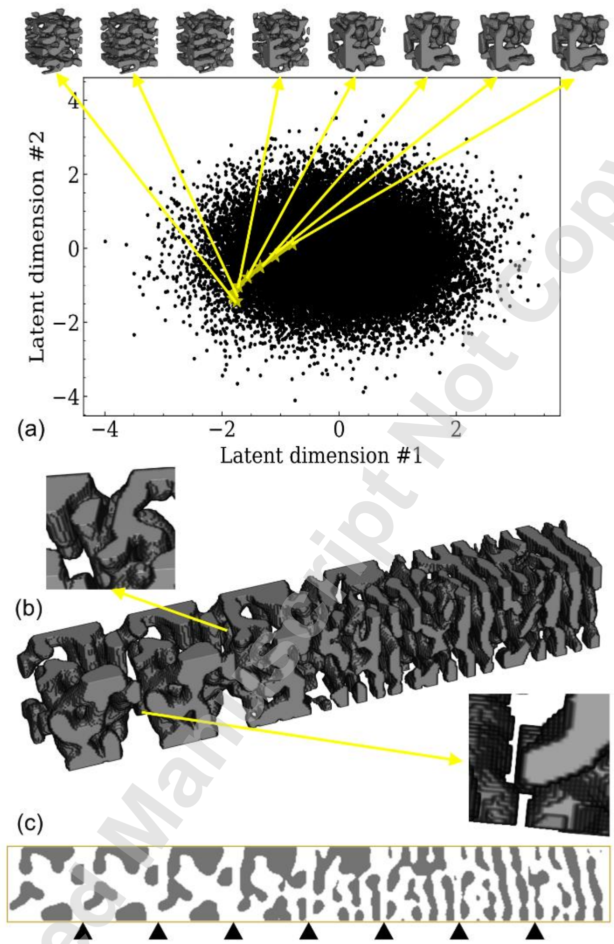

Figure 4: A functionally graded structure design by the deep generative modeling-based method. (a) A series of designs are generated along a certain path in two selected dimensions of the 256-dimensional latent space. Each star in the path is decoded into a microstructure unit. (b) A functionally graded structure design is created by assembling the microstructure units. Due to the discrete nature of the sampling process, non-smooth transitions can be observed at the interfaces among microstructure units. Two zoom-in views are shown to the non-smooth transitions. (c) Side view of the 3D functionally graded structure. The interfaces among adjacent units are marked by triangles.

3. CURVATUAL FUNCTIONAL-BASED METHOD

3.1 Microstructure representation by curvature functionals

Curvature functionals are capable of generating a variety of complex shapes and have been demonstrated as a powerful tool for designing bio-mimetic scaffold [50]. Curvature functionals employ a

Journal of Mechanical Design. Received June 20, 2023;
Accepted manuscript posted October 11, 2023. doi:10.1115/1.4063824

phase-field formulation to diffuse an approximation of a vast range of shape textures. The resulting approximation is used as a loss function, in conjunction with modern automatic differentiation optimizers, to generate geometries from a random field initialization. When compared to the phase-field [51, 52] and statistical functional approaches [25]，such as spinodal microstructures generated by Gaussian random field (GRF) [2, 53], curvature functionals have the ability to generate a broader range of topologies. These include laminar, spherical, pearly thin wall, and tube shapes, and are governed by seven generation parameters $\boldsymbol{a} = [a_{2,0}, a_{0,2}, a_{1,1}, a_{1,0}, a_{0,1}, a_{0,0}]$ and m_0. However, the mathematical meaning of the generation parameters is yet fully explored which limits the capability in directly using this method for inverse design. To address this limitation, we utilize the supervised learning method to establish the relation between generation parameters and properties to enable the property-driven microstructure design.

Gaussian curvature is a differential geometry measure of the curvature of a surface at a given point, which is defined as the production of the principal curvatures κ_1, κ_2 by

$$K = \kappa_1 \kappa_2. \tag{2}$$

The complex microstructure surface under constant volume is modelled as a curvature functional

$$\boldsymbol{F}(S) = \int_S p(\kappa_1, \kappa_2) dA. \tag{3}$$

where p is the second order polynomial of the principal curvatures of the entire surface S. p is restricted to the degree of 2, as it is efficient to generate topological features. The curvature functionals can be expanded as

$$\boldsymbol{F}(S) = \int_S \left(a_{2,0}\kappa_1{}^2 + a_{1,1}\kappa_1\kappa_2 + a_{0,2}\kappa_2{}^2 + a_{1,0}\kappa_1 + a_{0,1}\kappa_2 + a_{0,0}\right) dA = \int_S \left(\sum_{|\alpha|\leq 2} a_\alpha \, (\kappa_1\kappa_2)^\alpha\right) dA. \tag{4}$$

Generally, it is convenient to refine this kind of 2D surface functionals to scalar fields u in 3D volume by diffusion approximation. And the matrix field $\mathcal{M}_u^\epsilon$ is introduced as:

$$\mathcal{M}_u^\epsilon = -\epsilon \text{ Hess } u + \frac{W'(u)}{\epsilon} n_u \otimes n_u\,, \tag{5}$$

where Hess is the Hessian operator. And its trace is equal to

$$\text{Tr}\mathcal{M}_u^\epsilon = -\epsilon \Delta u + \frac{W'(u)}{\epsilon}. \tag{6}$$

Applied phase-field approximation and further simplification, the final representation of the phase-field $\mathcal{F}_\epsilon(u)$ can be written as

$$\mathcal{F}_\epsilon(u) = \int_\Omega \Big[\frac{a_{2,0}+a_{0,2}-a_{1,1}}{2\epsilon} \|\mathcal{M}_u^\epsilon\|^2 + \frac{a_{1,1}}{2\epsilon} (\text{Tr}\mathcal{M}_u^\epsilon)^2 + \frac{a_{2,0}-a_{0,2}}{2\epsilon} \text{Tr}\mathcal{M}_u^\epsilon \sqrt{(2\|\mathcal{M}_u^\epsilon\|^2 - (\text{Tr}\mathcal{M}_u^\epsilon)^2)^+} + \frac{a_{1,0}+a_{0,1}}{2} |\nabla u| \text{Tr}\mathcal{M}_u^\epsilon + \frac{a_{1,0}-a_{0,1}}{2} |\nabla u| \sqrt{(2\|\mathcal{M}_u^\epsilon\|^2 - (\text{Tr}\mathcal{M}_u^\epsilon)^2)^+} + a_{0,0}\epsilon |\nabla u|^2\Big] dx. \tag{7}$$

To implement the phase-field $\mathcal{F}_\epsilon(u)$ to generate microstructure geometries given a random initialization, a mass-preserving flow can be defined as

$$\dot{u} = \Delta \frac{\partial \mathrm{F}_\epsilon}{\partial u}. \tag{8}$$

This form can also be repressed as

$$u = \nabla \cdot A + m_0 \tag{9}$$

where $A\colon \Omega \to \mathbb{R}^3$ is a periodic vector field, and $m_0 \in \mathbb{R}$ is the desired value of the average $\bar{u}$ which also approximates the volume fraction by $\frac{m_0+1}{2}$. Finally, an energy function is defined as:

$$G_\epsilon(A) = \mathcal{F}_\epsilon(\nabla \cdot A + m_0)\,, \tag{10}$$

with a gradient of

$$\frac{\partial G_\epsilon}{\partial A}(A) = -\nabla \frac{\partial \mathrm{F}_\epsilon}{\partial u}(u). \tag{11}$$

Journal of Mechanical Design. Received June 20, 2023;
Accepted manuscript posted October 11, 2023. doi:10.1115/1.4063824

This energy function is used as the loss function with an auto-differentiation tool that iteratively optimizes u to evolve a random vector field A_0 until the energy function meets the convergence criterion, and this algorithm was implemented in a GPU implementation, curvatubes [50]. This iterative algorithm is shown in Figure 5(a). Empirically, A_0 can be drawn from a uniform distribution. Random initialization of the structure image in the curvature functional method results in diverse yet statistically equivalent stochastic reconstructions of microstructures that share the same input generation parameters $\boldsymbol{a}$ and m_0. Therefore, the generation variables can be considered as a statistical representation of an infinite set of random but statistically equivalent microstructures, which makes this method suitable for generating stochastic microstructure designs. Several examples of statistically equivalent microstructure samples generated from the same $\boldsymbol{a}$ vector is shown in Figure 5 (b~e). The final phase field, u, falls within a range of (-1, 1). It can also be binarized to represent various volume fraction levels or utilized to extract the zero-level set. Figure 5 (f) illustrates an example showcasing the geometric changes induced by volume fraction variations originating from the same phase field.

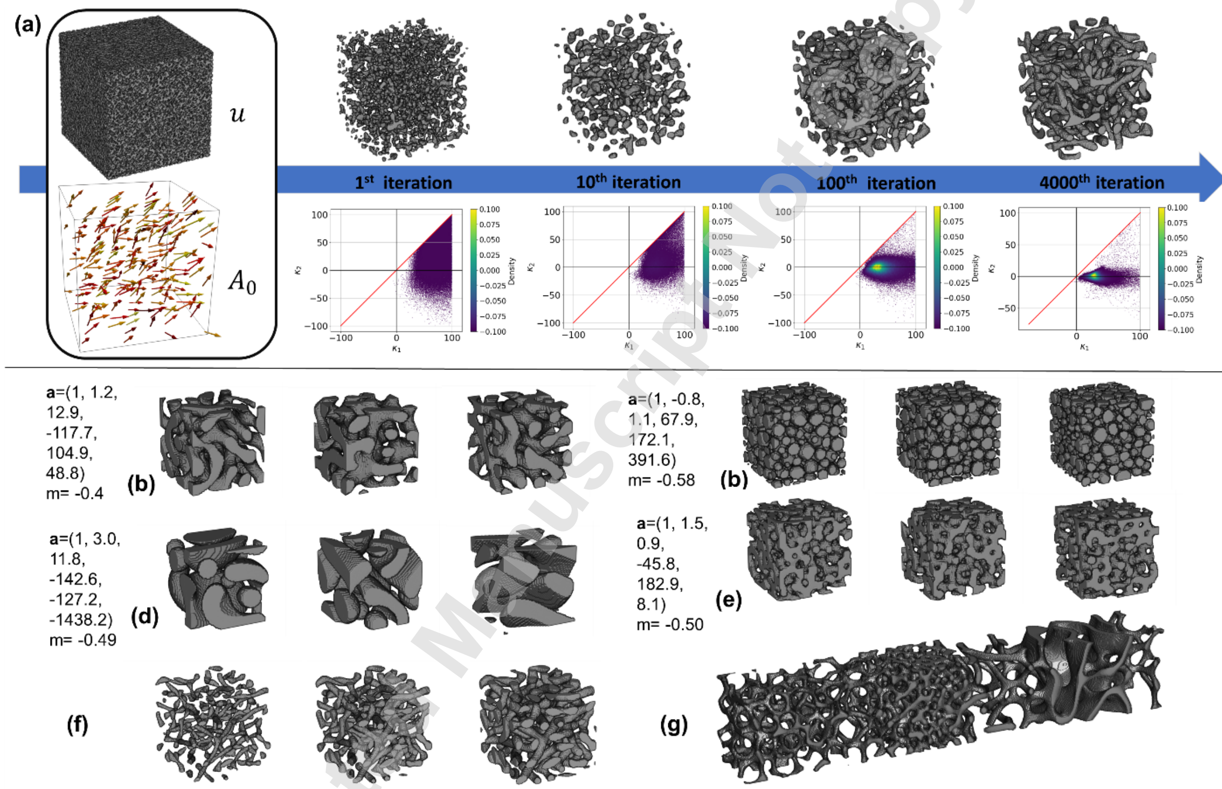

Figure 5: (a) The iterative generation process of curvature function method. The first block represents initial random vector field A_0 and corresponding phase field u computed by Equation 9. The binarized microstructures generated at iterations 1, 10, 100, and 4000 is represented in the first row, and the corresponding curvature diagrams at the second row shows distribution of the curvatures (κ_1, κ_2) on surface. (b)~(e) Design variable vectors and the corresponding statistically equivalent microstructure samples. Each row shows three stochastic samples of the same microstructure design and the corresponding generation parameters. (f) A phase-field u is binarized in a volume fraction of 0.3, 0.6, and 0.9. (g) A functionally graded structure obtained by the curvature functional-based method. It is created from continuous functions of the generation parameters $\boldsymbol{a}$.

Journal of Mechanical Design. Received June 20, 2023;
Accepted manuscript posted October 11, 2023. doi:10.1115/1.4063824

3.2 Property-driven microstructure design and generation of graded functional structure designs by curvature functionals

Following the flowchart in **Figure 1**, we propose a surrogate model-based optimization approach for microstructure design. The surrogate model of the relationship between the generation parameters $\boldsymbol{a}$ and material property is established using GP regression. It is to be noted that random but statistically equivalent microstructures will be generated for a given set of design variables. Therefore, we generated ten samples from ten fixed random initializations (A) for the same design variable vector, and then simulated the mechanical properties of all ten samples. We generated a total of 20,000 samples using 2,000 sets of generation parameters. Numerous synthetic examples are presented in Figure A.1(c), located in the appendix. Similar to the method presented in Section 2, we adopt GA and NSGA-II as the optimizers to solve the property-driven design problem. In the last step, the digital images of the microstructure designs are reconstructed based on the design variable vector $\boldsymbol{a}$.

Here we also investigated the curvature functional-based method's capability of generating functional graded structure designs. One advantage of the curvature functional method is that a smooth transition between different categories of microstructures can be easily obtained by varying the values of the generation parameters continuously. Figure 5(g) shows a functional graded design generated based on continuous functions of the generation parameters $\boldsymbol{a}$ along the longitudinal direction. Moreover, the curvature functional-based method offers the advantage of scalability, allowing it to reconstruct microstructure images with varying domain sizes and resolutions. Figure 6(a~c) visually illustrates this advantage by presenting three samples generated using identical design variable values but varying levels of resolution. Furthermore, the high-resolution reconstructions of microstructures with arbitrary sizes offer the convenience of seamless integration into macro-scale component geometries. This capability is exemplified in Figure 6(d~e), where the microstructure is infused into two macro-scale geometries resembling a human femur and a suspension arm, showcasing the ability to precisely fit the microstructure into complex shapes.

Manufacturing complex multiscale microstructures in a precise and economic method is still a challenge. Factors impacting manufacturing robustness, such as local defects and surface roughness, are vital considerations when evaluating manufacturability. In recent years, there have been significant improvements in additive manufacturing (AM) techniques. Techniques such as Stereolithography (SLA) [53] and extrusion additive manufacturing [54] have approved a great robustness in printing similar geometries shown in figure 6. If additive manufacturing is employed, it effectively eliminates manufacturing uncertainty and enables transition between different types of microstructures, though it comes with a higher cost. Conversely, alternative methods like the self-assembly of polymeric emulsions [17] are more cost-effective and high throughput volumes cross multiple scales, but are limited to producing specific types of microstructures.

Journal of Mechanical Design. Received June 20, 2023;
Accepted manuscript posted October 11, 2023. doi:10.1115/1.4063824

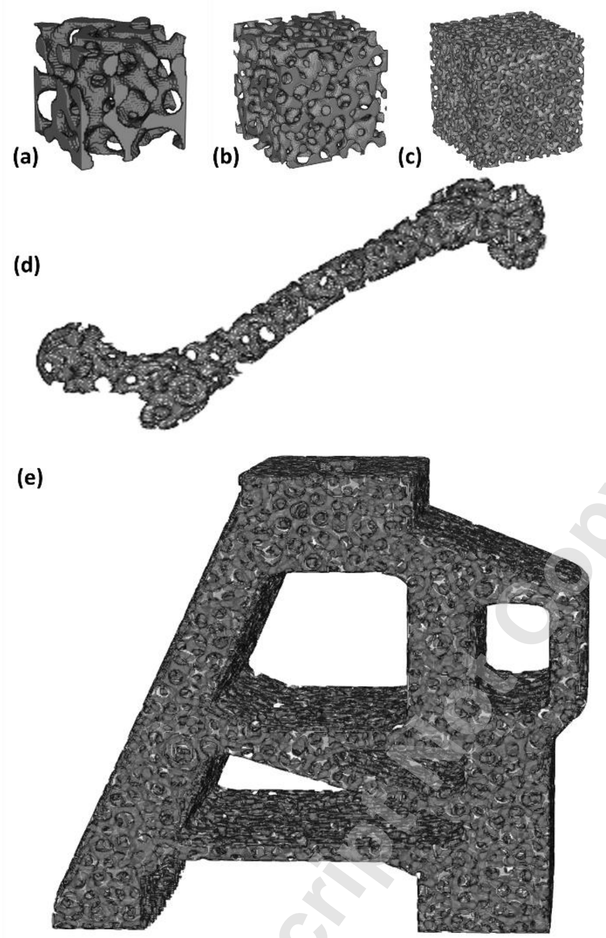

Figure 6: Scalability of the curvature functional-based method: microstructure designs generated from the same design variable vector $\boldsymbol{a}$ = [1, 2.8, 2, -10, -10, 25] and m_0 = -0.25 with sizes of (a) 64^3 (b) 128^3 (c) 256^3 voxels by the curvature functional-based method. Two macro-scale geometries in the shapes of (d) a human femur and (e) a suspension arm infused with microstructures generated with $\boldsymbol{a}$ = [1, 2.8, 2, -10, -10, 25] and m_0 = -0.25.

4. A COMPARATIVE STUDY WITH A DESIGN FOR STIFFNESS PROBLEM

In this section, we present a design case to compare the deep generative model-based and the curvature functional-based design representation methods in two aspects: the accuracy of the microstructure-property regressor and the performance of the optimal designs obtained with each method.

Here we define a multi-objective microstructure design problem that maximizes the Young's moduli along X-, Y-, and Z- directions. Design constraints are defined to guarantee close-to-isotropic designs, i.e., the differences between the maximum/minimum modulus and the median modulus of the three directions are within 3%. Therefore, the optimization problem can be formulated as

$$\max\ E_i(\boldsymbol{z})\ \text{ or} \max\ E_i(\boldsymbol{a}, m_0),\ i = \mathrm{X, Y, Z} \tag{12}$$

subject to:

$$\frac{|E_{\text{highest}} - E_{medium}|}{E_{medium}} < 3\% \tag{13}$$

$$\frac{|E_{\text{lowest}} - E_{medium}|}{E_{medium}} < 3\% \tag{14}$$

Journal of Mechanical Design. Received June 20, 2023;
Accepted manuscript posted October 11, 2023. doi:10.1115/1.4063824

When utilizing the VAE-based approach, the Euclidean distance of the solution latent vector $\boldsymbol{z}$ is employed to prevent the optimizer from searching in regions that cannot be decoded into meaningful images.

$$\frac{|\max\|\boldsymbol{z}_{train}\| - \|\boldsymbol{z}\||}{\max\|\boldsymbol{z}_{train}\|} < 3\% \quad (15)$$

where the $\max\|\boldsymbol{z}_{train}\|$ is the largest latent vector encoded from training data.

If using the curvature functional-based method, additional constraints are needed to guarantee the convergence of microstructure image reconstruction:

$$\max(u) > 0.1 \quad (16)$$

$$\min(u) < -0.1 \quad (17)$$

$$\text{discrepancy}(u) < 0.75 \quad (18)$$

where the discrepancy is a measurement of how much the scalar fields u deviate from a tanh profile phase field function [50]. As this research focuses on investigating the influence of microstructure morphology on the properties, the volume fraction is set as a constant (0.4).

As preparation for exploring the relationship between microstructure and the property of interest, in this case, elasticity, we performed finite element simulations on all microstructure samples by ABAQUS. The 0-1 matrices that represent the binary microstructure images are transformed into hexahedral meshes. The elastic modulus and Poisson's ratio of the 1 phase in the microstructure are $E_{Boron} = 379300$ MPa and $\gamma_{\text{Boron}} = 0.1$, whereas $E_{\text{Aluminum}} = 68300$ Mpa, $\gamma_{\text{Aluminum}} = 0.3$ for the 0 phase, where we consider only linear elasticity. Infinitesimal displacements are applied to the two surfaces along the axis of interest to stretch the microstructure, while the remaining four surfaces experience free traction. Young's moduli (E_x, E_y, E_z) in the X-, Y-, and Z-direction are calculated by dividing the average stress by the strain. The stress map and strain map with displacement boundary conditions are shown in **Figure 7**.

Journal of Mechanical Design. Received June 20, 2023;
Accepted manuscript posted October 11, 2023. doi:10.1115/1.4063824

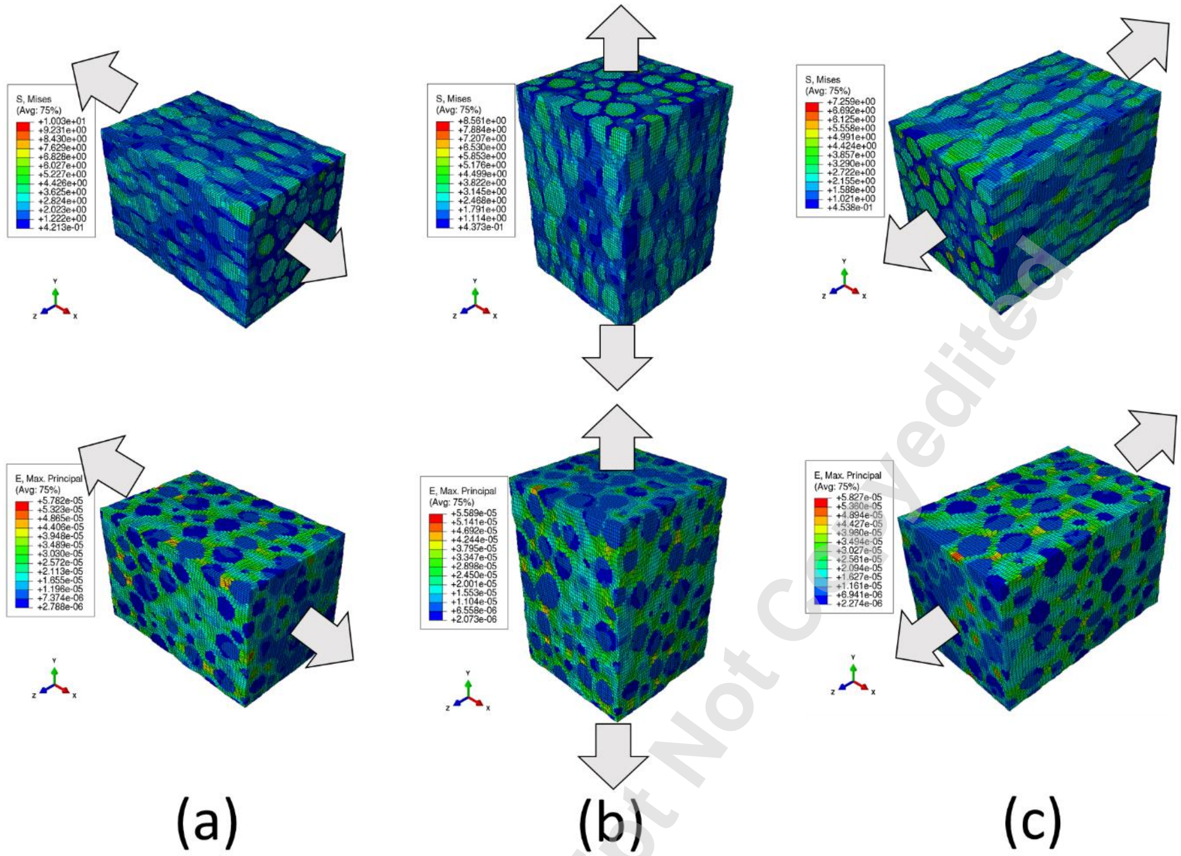

Figure 7: Elasticity property analysis on a microstructure for the maximum in-plane strain and the maximum von Mises stress in (a) X-direction, (b) Y-direction, and (c) Z-direction. The arrows indicate the direction of infinitesimal displacements.

The dimensionality of the design space has a strong impact on the predictability of the GP regressors. The design space generated by VAE has a dimensionality of 256. By contrast, the design space of the curvature functional-based method is only 7. More input variables indicate a potentially better capability to capture complex microstructure features, but practically, a high dimensional input space poses a significant challenge to establishing the design variable-property relationship by surrogate modeling because a lot more training data points are required to fully cover the input space. In **Table 1**, we present a comparison of three GP models: VAE latent space-based GP model with a dataset of 40000 samples, VAE latent space-based GP model with a dataset of 20000 samples, and curvature functional-based GP model with a dataset of 20000 samples. In each training, the dataset is split into a training set (90%) and a test set (10%). The model accuracy, R^2, is evaluated based on the test set. The curvature functional-based GP model has a higher accuracy, even when comparing with the VAE-based GP model that uses twice as many training data points. We also tested the neuron network (NN) regressor for both VAE and curvature functional method, the prediction accuracy and optimal design are very similar to the GP model, therefore, we keep GP in the rest of this manuscript. A table summarizing the accuracy of neuron network regressor can be found in **Table A.1** in appendix.

Table 1: Prediction accuracies of the GP regression models with the design spaces generated by the VAE-based method and the curvature functional-based method.

Journal of Mechanical Design. Received June 20, 2023;
Accepted manuscript posted October 11, 2023. doi:10.1115/1.4063824

Model (size of the dataset)	R^2 score		
	E_x	E_y	E_z
GP w/VAE (40000)	0.743	0.681	0.746
GP w/VAE (20000)	0.686	0.620	0.688
GP w/ curvature functional (20000)	0.811	0.803	0.775

Another point worth noting is that some combination of generation parameters in the curvature functional method may generate ill-posed geometric which may have zero level set and floating fragments, where such fragments can lead to unrealistic microstructures in composite material and porous material from both design and manufacturing perspectives. Therefore, three criteria, $\max(u)$, $\min(u)$, and discrepancy ratio, are required to identify ill-posed phase-field u during the optimization process. These three criteria must be included as inequality constraints in optimization to ensure successful reconstructions of the final microstructure designs. Experimentally, we observe that these three constraint functions limit the number of feasible designs significantly.

The Pareto frontiers obtained with the two methods are compared in **Figure 8**. The Pareto frontier is generated based on the virtual performances predicted using the trained machine learning model. Subsequently, verification simulations are performed to obtain the true performances of these designs. **Figure 8** is created based on the true performances of the obtained designs. Due to the predicted errors of the microstructure-property model, some of the obtained designs violate the design constraints of equivalent Young's moduli along three directions. For the VAE-based method, only 10% of the obtained designs in the Pareto frontier satisfy the design constraints. Among the feasible designs, we can hardly find designs that rank in the top 10% compared to the samples in the microstructure database, with respect to the properties of interest.

On the other hand, more than 70% percent of optimal designs found by the curvature functional approach meet the constraint of equivalent Young's moduli along three directions, according to the results of verification simulations. Furthermore, almost all of the feasible solution rank in the 10% compared to the samples in the microstructure database. **Figure 9 (a)~(d)** show several examples of the optimal designs obtained by the curvature functional-based method, and **Figure 9 (e) and (f)** show the optimal designs obtained by the VAE-based method.

Journal of Mechanical Design. Received June 20, 2023;
Accepted manuscript posted October 11, 2023. doi:10.1115/1.4063824

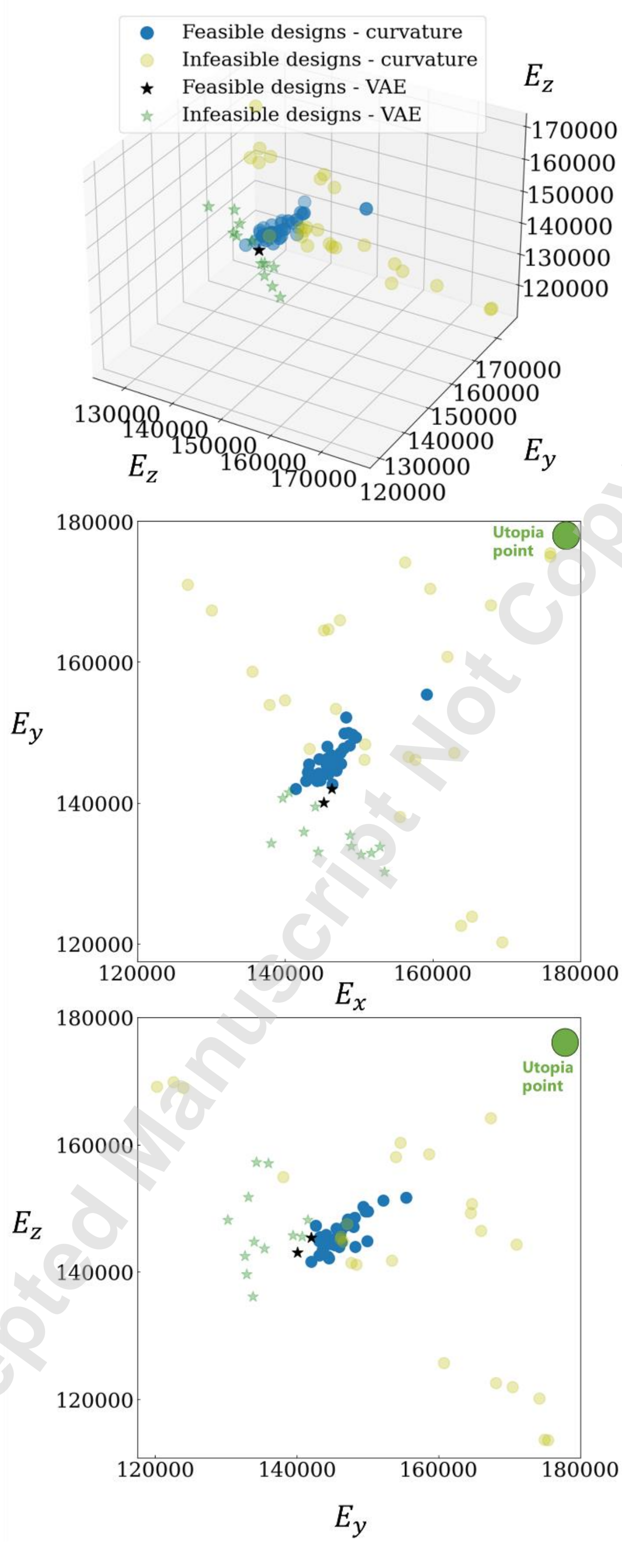

Figure 8: Pareto frontiers obtained by both design approaches. As there are three design objectives, one 3D view and two 2D views of the performance space are provided. The design objective is to maximize E_x, E_y, and E_z. The feasible design points are in dark colors and the infeasible design points are in light colors. The green dot indicates the location of the Utopia point.

Journal of Mechanical Design. Received June 20, 2023;
Accepted manuscript posted October 11, 2023. doi:10.1115/1.4063824

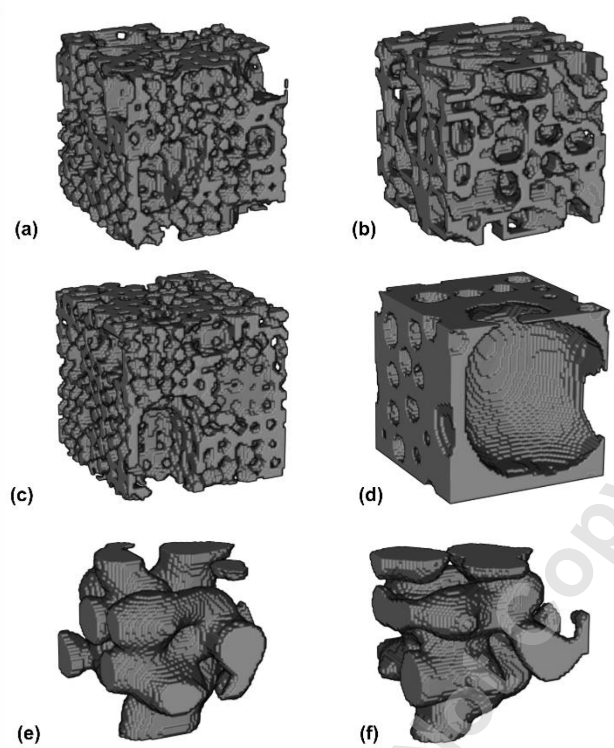

Figure 9: (a)~(d) Optimal designs from the curvature functional-based optimization approach. (a) $\boldsymbol{a}$ = [1, 3.987, 0.2194, 39.95, 198.4, 1431] and m_0 = -0.30. (b) $\boldsymbol{a}$ = [1, 3.990, 0.2933, 75.17, 199.3, -2060] and m_0 = -0.26. (c) $\boldsymbol{a}$ = [1, 3.990, 0.3354, 45.24, 197.4, 1422] and m_0 = -0.19. (d) $\boldsymbol{a}$ = [1, 3.925, 3.791, 36.08, 194.1, 2998] and m_0 = -0.43. (e) and (f) Two optimal designs from the VAE-based design approach.

5. UNDERSTANDING THE PROS AND CONS OF THE TWO DESIGN REPRESENTATION METHODS

As summarized in **Table 2**, the pros and cons of the deep generative modeling-based method and the curvature functional-based method are discussed in terms of seven criteria: computational cost, continuous transition in functionally graded structure design, scalability of the microstructure design, design diversity, dimensionality of the design space, and design performance.

Computational cost: To obtain a design space that embodies various categories of microstructures, the deep generative modeling-based approach requires significant computing resources for data generating and model training. On the other hand, the curvature functional-based method incurs minimal costs in defining the design space, while computing the viability constraints (Equation 16~18) during the optimization process is relatively computationally expensive.

Continuous transition in functionally graded structure design: When creating functionally graded structure designs, the curvature functional-based method can guarantee a smooth transition among various microstructure patterns. With the deep generative model-based method, the functionally graded structure design is created by assembling a series of microstructure units, which correspond to discrete points in the latent space. Therefore, a smooth transition between microstructure units cannot be guaranteed. This issue could potentially be mitigated (but not resolved) by applying circular spatial padding to the transposed convolutional layer in the deep generative model [55], but the impacts on reconstruction quality and computational complexity need further investigation.

Journal of Mechanical Design. Received June 20, 2023;
Accepted manuscript posted October 11, 2023. doi:10.1115/1.4063824

Scalability of the microstructure design: The deep generative models, which are trained on the images directly, cannot generate images with a wide range of sizes and resolutions. By contrast, the curvature functional-based method can easily map the design variables to an arbitrary domain size. In our experiments, the existing implementation of the curvature functional method can generate images with a maximum size of 512^3 using a single GPU with 48GB RAM.

Design diversity: The deep generative models have the advantage over the curvature functionals. Theoretically, the deep generative models can be extended to embody any type of microstructure (e.g., microstructures with triangular inclusions) as long as the training data are available. The curvature functionals can only generate microstructures with curved surfaces.

Dimensionality of the design space: The curvature functional-based method has the advantage in generating a low dimensional design space. Although we can also set the dimensionality of the VAE latent space to a very low value (e.g. 8, the same as the design space of the curvature functional method) by modifying the fully connected layers in encoder, in practice, it will lead to a much poorer reconstruction accuracy. The high dimensionality of the VAE latent space poses a significant challenge to establishing the microstructure-property relationship, as well as searching for the optimal microstructure designs in the design space.

Interpretability of statistical equivalency among stochastic microstructure designs: It is a unique requirement for stochastic microstructure design. From the perspective of statistical characterization and stochastic reconstruction, one "design" actually represents an infinite number of microstructure samples that are random but statistically equivalent. The design representation by curvature functional parameters can provide this capability. By contrast, in the latent space learned by the deep generative model, each point corresponds to one specific, unique microstructure image. The distance between the points is a measurement of the pixel-to-pixel similarity of the two images, instead of the similarity in the statistical sense. As shown in **Figure 10**, two statistically equivalent random particle microstructure samples are far apart in terms of the Euclidean distance in latent space, while the random particle microstructure #1 is closer to the quasi-random microstructure. Therefore, it is not possible to define statistical equivalency purely based on the distance in the latent space. We acknowledge the possibility of generating random but statistically equivalent microstructures by introducing empirical statistical descriptors into the loss function of deep generative models (e.g., GAN) [56], but then again, it loops back to our original research question: how to select proper descriptors for describing stochastic microstructures without compromising the design freedom.

Design performance: The performance of the optimal designs are influenced by two factors: the accuracy of the microstructure-property surrogate model, and the effectiveness of design exploration/searching in the design spaces generated by each method. Although the curvature functional-based method demonstrates better performances in the presented case study, we should be cautious to make a conclusion. In our previous work [41] and literature [57], it has been demonstrated that training the VAE and the latent variable-property regressor simultaneously can improve the property prediction accuracy. This paper focuses on the capability of learning a unified design space, so the simultaneously training of the latent space and the property repressor is out of scope and not included.

Journal of Mechanical Design. Received June 20, 2023;
Accepted manuscript posted October 11, 2023. doi:10.1115/1.4063824

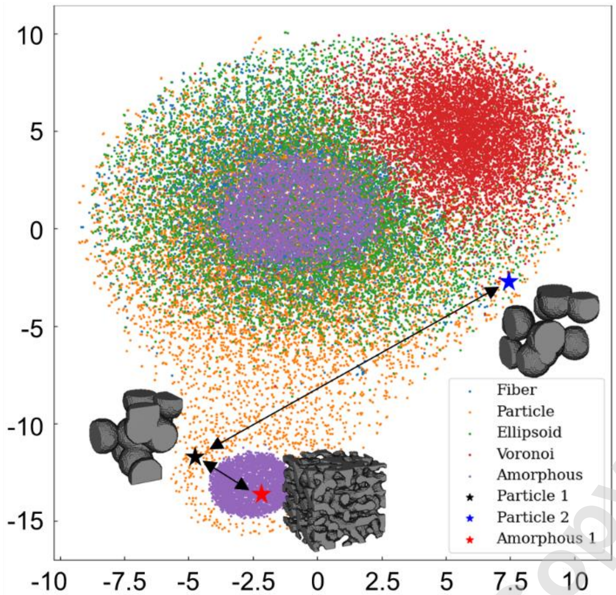

Figure 10: 2D *t*-SNE representations of VAE latent space. It is observed that the distance between two statistically equivalent random particle microstructures is larger than that between a random particle microstructure and an amorphous microstructure. Therefore, the Euclidean distance in the latent space cannot be used to identify statistically equivalent microstructures.

Table 2: Summary of the comparative study between the deep generative model-based and curvature functional-based methods. The criteria with * is only valid for the methods and case study presented in this paper.

Criteria	Deep generative model-based method	Curvature Functional-based method
Computational Cost	Significant computational resources for data generation and model training	Minimal cost in generating the design space, while computational expenses are incurred by computing the viability constraints during optimization
Continuous transition	Cannot guarantee smooth transitions between microstructure units in functionally graded structures	Smooth microstructure transition in functionally graded structures
Design scalability	Limited to specific sizes/resolutions	Arbitrary resolutions and domain sizes
Design diversity	Embodying any type of microstructure if the training data is available	Microstructures with curved surfaces only
* Dimensionality of the design space	High dimensionality poses challenges in establishing microstructure-property relationship and searching for optimal designs	Low-dimensional design space, compromising reconstruction accuracy

Journal of Mechanical Design. Received June 20, 2023;
Accepted manuscript posted October 11, 2023. doi:10.1115/1.4063824

Interpretability of statistical equivalency	Each design variable vector corresponds to a unique microstructure, not allowing statistical equivalence analysis	Each design variable vector represents random but statistical equivalent stochastic microstructures
* Design performance	Limited accuracy of the microstructure-property surrogate models and low design performances due to the high dimensionality of the design space	Lower dimensionality of the design space leads to better performance in presented case studies

6. CONCLUSION AND FUTURE WORK

In this paper, we proposed and compared two methods for generating a unified design space that embodies various categories of stochastic microstructures: the deep generative model-based method and the curvature functional-based method. For the deep generative model-based method, the latent space learned from a highly diversified microstructure database is employed as the microstructure design space. For the curvature functional-based method, the generation parameters in the functionals are used as microstructure design variables. We established surrogate models to predict the relationship between microstructure design variables and the properties of interest and conducted surrogate model-based optimization to design microstructures for desired properties. Furthermore, we applied the two methods to generate functionally graded structure designs. We present a comprehensive discussion and comparison of each method, outlining their respective advantages and drawbacks. This discussion serves to inform the design process for architecture and composite materials, aiding in the selection of an appropriate method based on the desired outcomes.

In our future work, we plan to test both methods on more engineering case studies to deepen our understanding of the strengths of each method. We are also aiming to further develop the current curvature functional method to generate multiscale microstructure fitting in an arbitrary domain. Another major limitation of this work is that the manufacturability analysis is not included. The purpose of this work is to establish a theoretical foundation for creating diverse geometries. While not currently integrated with the manufacturability analysis, the proposed methodology is an enabler for generating novel microstructure preliminary concepts, such as tailoring structural stochasticity for crashworthiness performances [41]. The development of a manufacturability-conscious design framework will be a focus of future efforts.

APPENDIX

Journal of Mechanical Design. Received June 20, 2023;
Accepted manuscript posted October 11, 2023. doi:10.1115/1.4063824

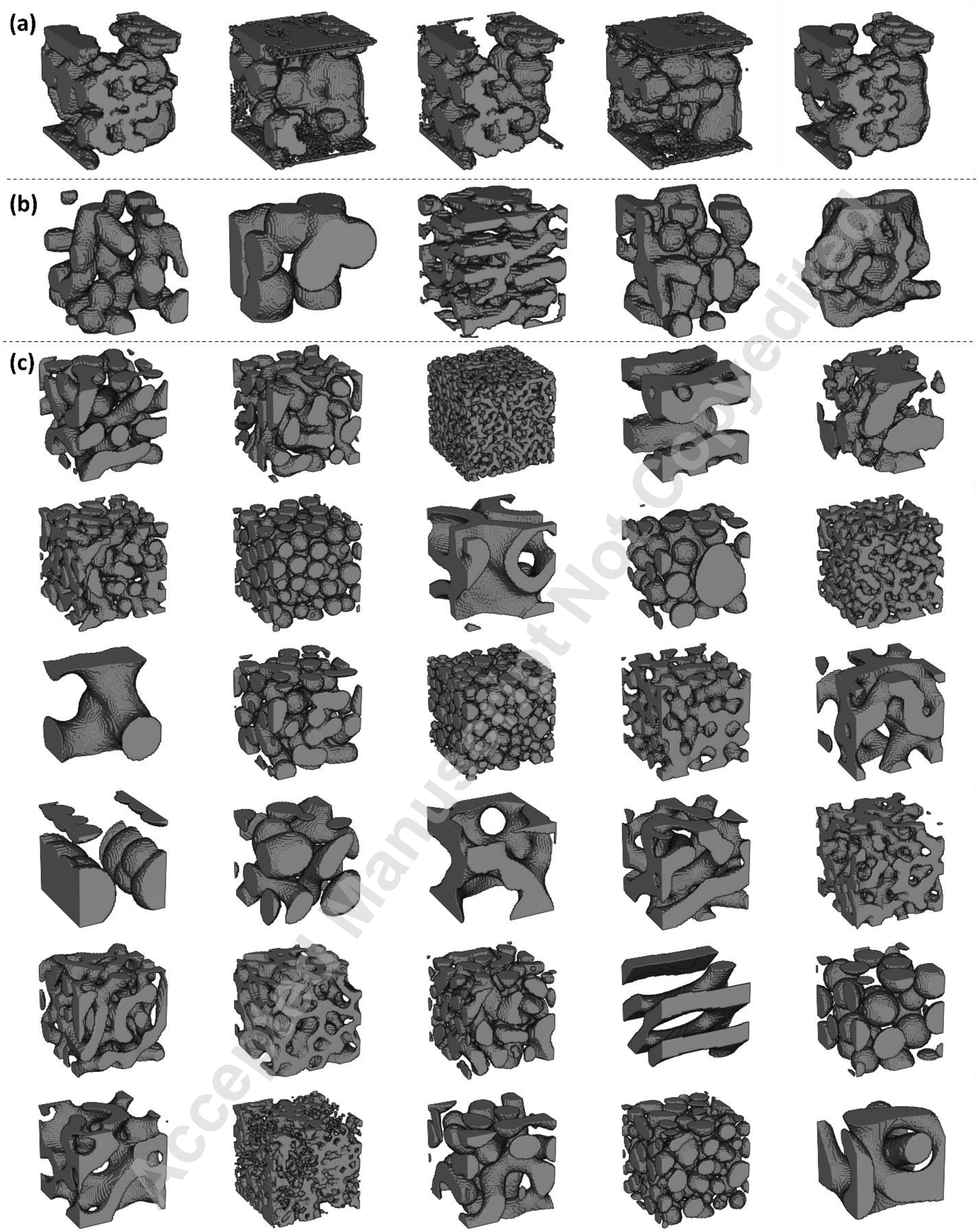

Figure A.1: Synthetic microstructures generated by (a) WGAN and (b) VAE using samples drawn from a standard Normal distribution. (c) Synthetic microstructures in the curvature-functional method dataset.

Journal of Mechanical Design. Received June 20, 2023;
Accepted manuscript posted October 11, 2023. doi:10.1115/1.4063824

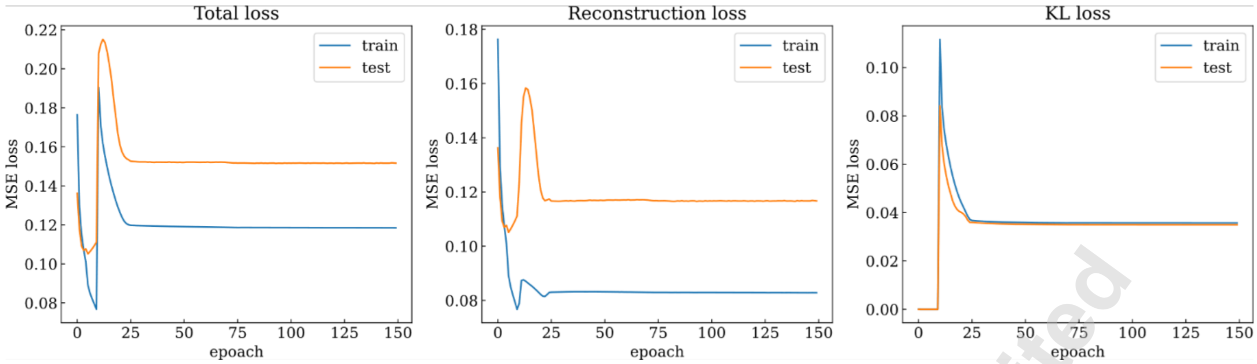

Figure A.2: Training history of VAE model using monotonic annealing schedule for KL loss.

Table A.1: Prediction accuracies of the neuron network regression models with the design spaces generated by the VAE-based method and the curvature functional-based method.

Model (size of the dataset)	R^2 score		
	E_x	E_y	E_z
NN w/VAE (40000)	0.782	0.733	0.760
NN w/ Curvature (20000)	0.781	0.795	0.755

Table A.2: Reconstruction accuracies for each catalog of microstructure in the test set for the posted VAE model.

Model	MSE loss					
	Overall	Fibers	Particles	Ellipsoids	node-edge network	amorphous
VAE	0.1167	0.0954	0.1044	0.0778	0.1261	0.1793

ACKNOWLEDGEMENT

The authors gratefully acknowledge financial support from the National Science Foundation (CAREER Award CMMI-2142290). L.X. sincerely thanks the insightful discussions with Anna Song at Imperial College London.

REFERENCES

[1] Meyer, P. P., Bonatti, C., Tancogne-Dejean, T., and Mohr, D., 2022, "Graph-based metamaterials: Deep learning of structure-property relations," Materials & Design, 223, p. 111175.
[2] Kumar, S., Tan, S., Zheng, L., and Kochmann, D. M., 2020, "Inverse-designed spinodoid metamaterials," npj Computational Materials, 6(1), p. 73.
[3] Wang, Z., Xian, W., Baccouche, M. R., Lanzerath, H., Li, Y., and Xu, H., 2022, "Design of phononic bandgap metamaterials based on gaussian mixture beta variational autoencoder and iterative model updating," Journal of Mechanical Design, 144(4), p. 041705.
[4] Kim, Y., Park, H. K., Jung, J., Asghari-Rad, P., Lee, S., Kim, J. Y., Jung, H. G., and Kim, H. S., 2021, "Exploration of optimal microstructure and mechanical properties in continuous microstructure space using a variational autoencoder," Materials & Design, 202, p. 109544.
[5] Guo, M., Jiang, J., Shen, Z., Lin, Y., Nan, C.-W., and Shen, Y., 2019, "High-energy-density ferroelectric polymer nanocomposites for capacitive energy storage: enhanced breakdown strength and improved discharge efficiency," Materials Today, 29, pp. 49-67.
[6] Ye, Q., Liu, Y., Lin, H., Li, M., and Yang, H., 2012, "Multi-band metamaterial absorber made of multi-gap SRRs structure," Applied Physics A, 107, pp. 155-160.

Journal of Mechanical Design. Received June 20, 2023;
Accepted manuscript posted October 11, 2023. doi:10.1115/1.4063824

[7] Yaji, K., Yamasaki, S., and Fujita, K., 2022, "Data-driven multifidelity topology design using a deep generative model: Application to forced convection heat transfer problems," Computer Methods in Applied Mechanics and Engineering, 388, p. 114284.
[8] Du, P., Zebrowski, A., Zola, J., Ganapathysubramanian, B., and Wodo, O., 2018, "Microstructure design using graphs," npj Computational Materials, 4(1), p. 50.
[9] Li, Y., Chen, Z., Su, L., Chen, W., Jin, X., and Xu, H., 2018, "Stochastic reconstruction and microstructure modeling of SMC chopped fiber composites," Composite Structures, 200, pp. 153-164.
[10] Chen, Z., Huang, T., Shao, Y., Li, Y., Xu, H., Avery, K., Zeng, D., Chen, W., and Su, X., 2018, "Multiscale finite element modeling of sheet molding compound (SMC) composite structure based on stochastic mesostructure reconstruction," Composite Structures, 188, pp. 25-38.
[11] Tucho, W. M., Lysne, V. H., Austbø, H., Sjolyst-Kverneland, A., and Hansen, V., 2018, "Investigation of effects of process parameters on microstructure and hardness of SLM manufactured SS316L," Journal of Alloys and Compounds, 740, pp. 910-925.
[12] Wang, S., Ning, J., Zhu, L., Yang, Z., Yan, W., Dun, Y., Xue, P., Xu, P., Bose, S., and Bandyopadhyay, A., 2022, "Role of porosity defects in metal 3D printing: Formation mechanisms, impacts on properties and mitigation strategies," Materials Today.
[13] Tran‐Phu, T., Daiyan, R., Ta, X. M. C., Amal, R., and Tricoli, A., 2022, "From Stochastic Self‐Assembly of Nanoparticles to Nanostructured (Photo) Electrocatalysts for Renewable Power‐to‐X Applications via Scalable Flame Synthesis," Advanced Functional Materials, 32(13), p. 2110020.
[14] Xu, H., Zhu, J., Finegan, D. P., Zhao, H., Lu, X., Li, W., Hoffman, N., Bertei, A., Shearing, P., and Bazant, M. Z., 2021, "Guiding the design of heterogeneous electrode microstructures for Li‐ion batteries: microscopic imaging, predictive modeling, and machine learning," Advanced Energy Materials, 11(19), p. 2003908.
[15] Guell Izard, A., Bauer, J., Crook, C., Turlo, V., and Valdevit, L., 2019, "Ultrahigh energy absorption multifunctional spinodal nanoarchitectures," Small, 15(45), p. 1903834.
[16] Yang, Z., Li, X., Catherine Brinson, L., Choudhary, A. N., Chen, W., and Agrawal, A., 2018, "Microstructural materials design via deep adversarial learning methodology," Journal of Mechanical Design, 140(11).
[17] Portela, C. M., Vidyasagar, A., Krödel, S., Weissenbach, T., Yee, D. W., Greer, J. R., and Kochmann, D. M., 2020, "Extreme mechanical resilience of self-assembled nanolabyrinthine materials," Proceedings of the National Academy of Sciences, 117(11), pp. 5686-5693.
[18] Li, Y., Chen, Z., Xu, H., Dahl, J., Zeng, D., Mirdamadi, M., and Su, X., 2017, "Modeling and simulation of compression molding process for sheet molding compound (SMC) of chopped carbon fiber composites," SAE International Journal of Materials and Manufacturing, 10(2), pp. 130-137.
[19] Do, Q. T., Nguyen, C. H. P., and Choi, Y., 2021, "Homogenization-based optimum design of additively manufactured Voronoi cellular structures," Additive Manufacturing, 45, p. 102057.
[20] Jiao, Y., Stillinger, F., and Torquato, S., 2007, "Modeling heterogeneous materials via two-point correlation functions: Basic principles," Physical Review E, 76(3), p. 031110.
[21] Jiao, Y., Stillinger, F. H., and Torquato, S., 2008, "Modeling heterogeneous materials via two-point correlation functions. II. Algorithmic details and applications," Phys Rev E, 77(3).
[22] Torquato, S., 2010, "Optimal design of heterogeneous materials," Annu Rev Mater Res, 40, pp. 101-129.
[23] Zhang, Y., Yan, M., Wan, Y., Jiao, Z., Chen, Y., Chen, F., Xia, C., and Ni, M., 2019, "High-throughput 3D reconstruction of stochastic heterogeneous microstructures in energy storage materials," npj Computational Materials, 5(1), pp. 1-8.
[24] Yu, S., Wang, C., Zhang, Y., Dong, B., Jiang, Z., Chen, X., Chen, W., and Sun, C., 2017, "Design of non-deterministic quasi-random nanophotonic structures using Fourier space representations," Scientific reports, 7(1), pp. 1-10.
[25] Iyer, A., Dulal, R., Zhang, Y., Ghumman, U. F., Chien, T., Balasubramanian, G., and Chen, W., 2020, "Designing anisotropic microstructures with spectral density function," Comp Mater Sci, 179, p. 109559.
[26] Grigoriu, M., 2003, "Random field models for two-phase microstructures," J Appl Phys, 94(6), pp. 3762-3770.
[27] Levina, E., and Bickel, P. J., 2006, "Texture synthesis and nonparametric resampling of random fields," The Annals of Statistics, 34(4), pp. 1751-1773.
[28] Advani, S. G., and Tucker III, C. L., 1987, "The use of tensors to describe and predict fiber orientation in short fiber composites," Journal of rheology, 31(8), pp. 751-784.
[29] Xu, H., Liu, R., Choudhary, A., and Chen, W., 2015, "A machine learning-based design representation method for designing heterogeneous microstructures," Journal of Mechanical Design, 137(5), p. 051403.

Journal of Mechanical Design. Received June 20, 2023;
Accepted manuscript posted October 11, 2023. doi:10.1115/1.4063824

[30] Xu, H., Dikin, D. A., Burkhart, C., and Chen, W., 2014, "Descriptor-based methodology for statistical characterization and 3D reconstruction of microstructural materials," Computational Materials Science, 85, pp. 206-216.
[31] Li, Y., Xu, H., Lai, W.-J., Li, Z., and Su, X., 2019, "A Multiscale Material Modeling Approach to Predict the Mechanical Properties of Powder Bed Fusion (PBF) Metal with Consideration of Microstructure Uncertainties," Fourth ASTM Symposium on Structural Integrity of Additive Manufactured Materials & PartsOxon Hill, Maryland, USA.
[32] Tan, R. K., Zhang, N. L., and Ye, W., 2020, "A deep learning–based method for the design of microstructural materials," Structural and Multidisciplinary Optimization, 61, pp. 1417-1438.
[33] Bostanabad, R., 2020, "Reconstruction of 3D microstructures from 2D images via transfer learning," Computer-Aided Design, 128, p. 102906.
[34] Dahari, A., Kench, S., Squires, I., and Cooper, S. J., 2023, "Fusion of complementary 2D and 3D mesostructural datasets using generative adversarial networks," Advanced Energy Materials, 13(2), p. 2202407.
[35] Noguchi, S., and Inoue, J., 2021, "Stochastic characterization and reconstruction of material microstructures for establishment of process-structure-property linkage using the deep generative model," Physical Review E, 104(2), p. 025302.
[36] Kench, S., and Cooper, S. J., 2021, "Generating three-dimensional structures from a two-dimensional slice with generative adversarial network-based dimensionality expansion," Nature Machine Intelligence, 3(4), pp. 299-305.
[37] Cang, R., Xu, Y., Chen, S., Liu, Y., Jiao, Y., and Yi Ren, M., 2017, "Microstructure representation and reconstruction of heterogeneous materials via deep belief network for computational material design," Journal of Mechanical Design, 139(7).
[38] Jung, J., Yoon, J. I., Park, H. K., Jo, H., and Kim, H. S., 2020, "Microstructure design using machine learning generated low dimensional and continuous design space," Materialia, 11, p. 100690.
[39] Lim, H. J., Lee, K.-H., and Yun, G. J., 2023, "Microstructure Design of Multifunctional Particulate Composite Materials using Conditional Diffusion Models," arXiv preprint arXiv:2301.09051.
[40] Deng, S., Mora, C., Apelian, D., and Bostanabad, R., 2023, "Data-Driven Calibration of Multifidelity Multiscale Fracture Models Via Latent Map Gaussian Process," Journal of Mechanical Design, 145(1), p. 011705.
[41] Xu, L., Hoffman, N., Wang, Z., and Xu, H., 2022, "Harnessing structural stochasticity in the computational discovery and design of microstructures," Materials & Design, 223, p. 111223.
[42] Li, Y., Chen, W., Xu, H., and Jin, X., 2016, "3D representative volume element reconstruction of fiber composites via orientation tensor and substructure features," 31st Annual Technical Conference of the American Society for Composites, American Society for Composites.
[43] Hoffman, N., Lee, J., Li, W., Zhu, J., and Xu, H., 2021, "A Stochastic Microstructure Reconstruction-Based Mechanical and Transport Modeling Approachfor Learning the Microstructure-Property Relationship of Li-Ion Battery Graphite Anodes," 239th ECS meetingDigital Meeting.
[44] Gulrajani, I., Ahmed, F., Arjovsky, M., Dumoulin, V., and Courville, A. C., 2017, "Improved training of wasserstein gans," Advances in neural information processing systems, 30.
[45] Fu, H., Li, C., Liu, X., Gao, J., Celikyilmaz, A., and Carin, L., 2019, "Cyclical annealing schedule: A simple approach to mitigating kl vanishing," arXiv preprint arXiv:1903.10145.
[46] Cang, R., Li, H., Yao, H., Jiao, Y., and Ren, Y., 2018, "Improving direct physical properties prediction of heterogeneous materials from imaging data via convolutional neural network and a morphology-aware generative model," Comp Mater Sci, 150, pp. 212-221.
[47] Dilokthanakul, N., Mediano, P. A., Garnelo, M., Lee, M. C., Salimbeni, H., Arulkumaran, K., and Shanahan, M., 2016, "Deep unsupervised clustering with gaussian mixture variational autoencoders," arXiv preprint arXiv:1611.02648.
[48] Deb, K., Pratap, A., Agarwal, S., and Meyarivan, T., 2002, "A fast and elitist multiobjective genetic algorithm: NSGA-II," IEEE transactions on evolutionary computation, 6(2), pp. 182-197.
[49] Shoemake, K., "Animating rotation with quaternion curves," Proc. Proceedings of the 12th annual conference on Computer graphics and interactive techniques, pp. 245-254.
[50] Song, A., 2022, "Generation of tubular and membranous shape textures with curvature functionals," Journal of Mathematical Imaging and Vision, 64(1), pp. 17-40.
[51] Geslin, P.-A., McCue, I., Gaskey, B., Erlebacher, J., and Karma, A., 2015, "Topology-generating interfacial pattern formation during liquid metal dealloying," Nature communications, 6(1), p. 8887.
[52] Montes de Oca Zapiain, D., Stewart, J. A., and Dingreville, R., 2021, "Accelerating phase-field-based microstructure evolution predictions via surrogate models trained by machine learning methods," npj Computational Materials, 7(1), p. 3.

Journal of Mechanical Design. Received June 20, 2023;
Accepted manuscript posted October 11, 2023. doi:10.1115/1.4063824

[53] Senhora, F. V., Sanders, E. D., and Paulino, G. H., 2022, "Optimally‐Tailored Spinodal Architected Materials for Multiscale Design and Manufacturing," Advanced Materials, 34(26), p. 2109304.
[54] Jiang, J., Zhai, X., Zhang, K., Jin, L., Lu, Q., Shen, Z., and Liao, W.-H., 2023, "Low-melting-point alloys integrated extrusion additive manufacturing," Additive Manufacturing, p. 103633.
[55] Gayon-Lombardo, A., Mosser, L., Brandon, N. P., and Cooper, S. J., 2020, "Pores for thought: generative adversarial networks for stochastic reconstruction of 3D multi-phase electrode microstructures with periodic boundaries," npj Computational Materials, 6(1), pp. 1-11.
[56] Zhang, F., Teng, Q., Chen, H., He, X., and Dong, X., 2021, "Slice-to-voxel stochastic reconstructions on porous media with hybrid deep generative model," Comp Mater Sci, 186, p. 110018.
[57] Wang, L., Chan, Y.-C., Ahmed, F., Liu, Z., Zhu, P., and Chen, W., 2020, "Deep generative modeling for mechanistic-based learning and design of metamaterial systems," Comput Method Appl M, 372, p. 113377.